



Published in final edited form as:

Cell Rep. 2022 November 29; 41(9): 111736. doi:10.1016/j.celrep.2022.111736.

Spatial transcriptomics demonstrates the role of CD4 T cells in effector CD8 T cell differentiation during chronic viral infection

Paytsar Topchyan^{1,2}, Ryan Zander^{1,3}, Moujtaba Y. Kasmani^{1,2}, Christine Nguyen^{1,2}, Ashley Brown^{1,2}, Siying Lin^{1,2}, Robert Burns¹, Weiguo Cui^{1,2,4,5,*}

¹Blood Research Institute, Versiti Wisconsin, 8727 West Watertown Plank Road, Milwaukee, WI 53213, USA

²Department of Microbiology and Immunology, Medical College of Wisconsin, 8701 West Watertown Plank Road, Milwaukee, WI 53226, USA

³Present address: Department of Microbiology and Immunology, University of Iowa, 431 Newton Road, Iowa City, IA 52242, USA

⁴Present address: Department of Pathology, Northwestern University, Feinberg School of Medicine, 303 E Chicago Ave, Chicago, IL 60611, USA

⁵Lead contact

SUMMARY

CD4 T cell help is critical to sustain effector CD8 T cell responses during chronic infection, notably via T follicular helper (Tfh)-derived interleukin-21 (IL-21). Conversely, CD4 depletion results in severe CD8 T cell dysfunction and lifelong viremia despite CD4 T cell reemergence following transient depletion. These observations suggest that repopulating CD4 subsets are functionally or numerically insufficient to orchestrate a robust CD8 response. We utilize spatial transcriptomics and single-cell RNA sequencing (scRNA-seq) to investigate CD4 T cell heterogeneity under CD4-replete and -deplete conditions and explore cellular interactions during chronic infection. Although IL-21-producing Tfh cells repopulate following transient CD4 depletion, they are outnumbered by immunomodulatory CD4 T cells. Moreover, the splenic architecture appears perturbed, with decreases in white pulp regions, coinciding with germinal center losses. These disruptions in splenic architecture are associated with diminished Tfh and progenitor CD8 T cell colocalization, providing a potential mechanism for impaired progenitor-to-effector CD8 T cell differentiation during “un-helped” conditions.

This is an open access article under the CC BY-NC-ND license (<http://creativecommons.org/licenses/by-nc-nd/4.0/>).

*Correspondence: weiguo.cui@northwestern.edu.

AUTHOR CONTRIBUTIONS

Conceptualization and methodology, P.T. and W.C.; investigation, P.T., C.N., and R.Z. with assistance from M.Y.K., A.B., and S.L.; formal analysis, P.T. with assistance from M.Y.K. and R.B.; writing – original draft, P.T.; writing – review & editing, M.Y.K., R.Z., W.C., A.B., and S.L.; funding acquisition and supervision, W.C.

DECLARATION OF INTERESTS

The authors declare no competing interests.

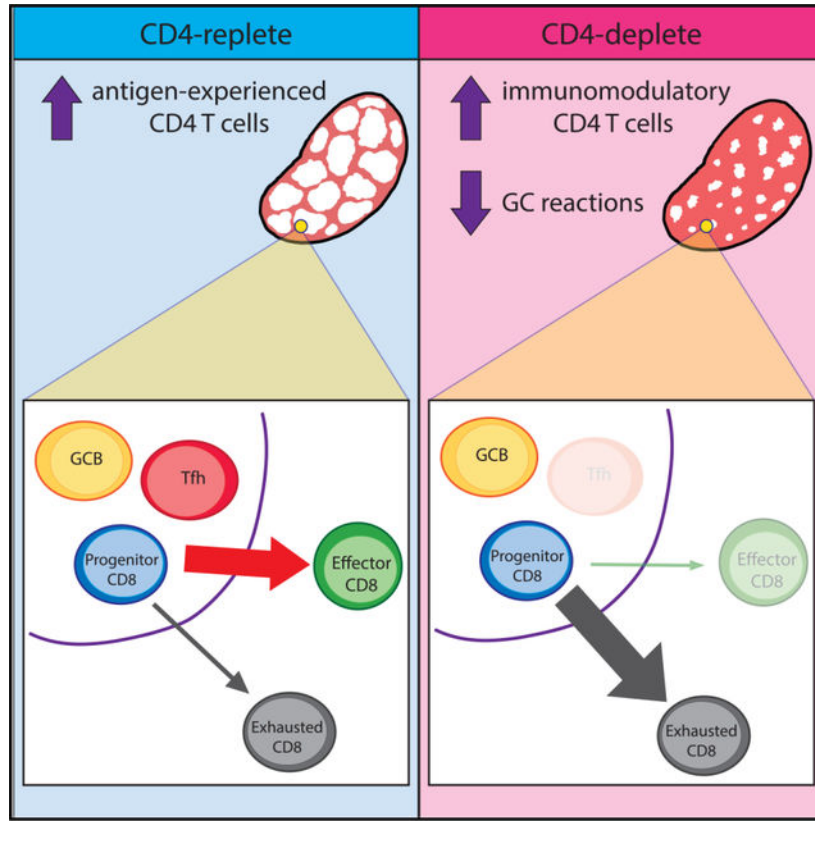
SUPPLEMENTAL INFORMATION

Supplemental information can be found online at <https://doi.org/10.1016/j.celrep.2022.111736>.

In brief

To address why repopulated CD4 T cells after initial depletion fail to rescue the functional effector CD8 T cells during chronic LCMV infection, Topchyan et al. apply spatial transcriptomics and find loss of Tfh cells and their interaction with progenitor CD8 T cells and B cells as a possible reason.

Graphical Abstract



INTRODUCTION

CD4 and CD8 T cells are critical in the immune response, namely against pathogenic infections and cancer. Although it is known that CD4 T cells provide help to CD8 T cells, precisely when, where, and by what mechanisms this “help” takes place continue to be of great interest.¹ During chronic infection, CD4 T cells play a critical role in sustaining the effector function of CD8 T cells.^{2–4} Notably, several recent studies have identified that CD8 T cells responding to chronic viral infection are heterogeneous and can be subset into at least three phenotypically, functionally, and epigenetically distinct subsets. Progenitor $Ly108^{hi}$ $TCF-1^{hi}$ CD8 T cells, which are a precursor population with self-renewing abilities, can give rise to either terminally differentiated exhausted $PD-1^{hi}$ CD8 T cells or effector CX_3CR1^{hi} CD8 T cells, which maintain their functional capacity to control viral infection.^{3–12} In particular, effector CD8 T cells arise when CD4 T cells help in the form of interleukin-21 (IL-21) production.^{3,13} Conversely, if CD4 T cell help is

absent, CD8 T cells enter a dysfunctional state, losing their capacity for viral control.^{2,14,15} Thus, developing a clearer understanding of how CD4 T cells aid in progenitor CD8 T cell differentiation has significant therapeutic potential.

In response to chronic viral infection, CD4 T cells steadily increase their production of IL-21,¹⁶ which serves as a critical mechanism by which CD4 T cells sustain effector CD8 T cell responses during prolonged infection.¹⁷⁻¹⁹ Importantly, we recently identified that BATF, a transcription factor (TF) downstream of IL-21 signaling,¹⁶ is essential for facilitating progenitor-to-effector CD8 T cell transition,²⁰ thereby providing mechanistic insight into how IL-21 signaling imparts a cytotoxic differentiation program in CD8 T cells. However, despite this apparent role for CD4 T cell-secreted IL-21, whether or not a particular IL-21-producing T helper cell subset is instrumental in facilitating this CD8 T cell differentiation process remained largely unclear.^{3,4,13} Notably, our latest work demonstrates that T follicular helper (Tfh) cells produce the highest amounts of IL-21 during lymphocytic choriomeningitis virus (LCMV) clone 13 (Cl13) infection and that Tfh-derived IL-21 is critical to sustain effector CD8 T cell responses and viral control during chronic infection.²¹ Additionally, Tfh cell-derived IL-21 is also necessary for germinal center responses; the absence of IL-21 results in impaired germinal center maintenance, reduced B cell affinity maturation, and isotype class switching.²²⁻²⁴ Therefore, CD4 T cell help during chronic infection is critical for CD8 T cell-mediated and humoral responses against persistent viral infection. Nevertheless, how this interaction between virus-specific Tfh cells and CD8 T cells is achieved spatially remains unclear.

It is well-established that LCMV Cl13 infection induces immunopathology, resulting in disruption of the splenic architecture in a CD8 T cell-dependent manner.^{25,26} LCMV causes severe destruction of organized lymphoid follicular structures, particularly in secondary lymphoid organs.²⁷ This is due to LCMV infection of fibroblastic reticular cells, which form conduit networks that are important for lymphoid architecture and function.²⁶ Although CD8 T cells may be responsible for disruption of the splenic architecture and other lymphoid tissues early on in infection,^{26,28} follicular integrity appears to be restored during later stages of chronic infection.²⁸ Regulatory T cells (Tregs) may play an important role in dampening the excessive activation of the immune system to limit the tissue disruption that results during chronic viral infection,²⁹ which supports the modulatory role of Tregs in CD8 T cell exhaustion.³⁰ Although ablation of Tregs limits CD8 T cell expansion, rescue of CD8 T cells from exhaustion appears to depend on B7 costimulation and CD4 T cell help.³⁰ Therefore, understanding the key subsets of CD4 T cells that shape the trajectory of the CD8 T response during chronic infection is important in elucidating CD8 T cell differentiation and harnessing this knowledge to develop effective therapeutics.

Spatial transcriptomics (ST) combined with single-cell RNA sequencing (scRNA-seq) allow us to study both cellular diversity and heterogeneity and to explore cellular localization and potential interaction between subsets. We utilized both of these techniques to characterize CD4 T cell repopulation following CD4 T cell depletion and study how IL-21-producing CD4 T cells may colocalize with progenitor CD8 T cells within the splenic architecture. Our findings suggest that although IL-21-producing Tfh CD4 T cells do repopulate, they are highly outnumbered by other immunomodulatory CD4 T cells such as Tregs. In addition, a

lack of CD4 T cell help during chronic viral infection may result in disruption of the splenic architecture, which prevents the colocalization of Tfh and progenitor CD8 T cells, thereby impairing progenitor-to-effector CD8 T cell differentiation.

RESULTS

IL-21-producing CD4 T cells repopulate following CD4 T cell depletion

Depletion of CD4 T cells before LCMV C113 infection precludes the development of effector CD8 T cells and is known to result in severe CD8 T cell dysfunction and lifelong viremia.² However, given that CD4 T cells are capable of repopulating the T cell pool following transient CD4 T cell depletion,³¹ this brings us to question whether the CD4 T cells that reemerge after depletion are either phenotypically distinct and functionally inferior (such as lower IL-21 expression) or if this failure to generate protective CD8 T cell responses is simply due to numerical deficiencies in the CD4 T cell compartment. To determine whether IL-21-producing CD4 T cells are able to repopulate in LCMV C113 chronically infected mice following depletion of CD4 T cells, IL-21-turbo red fluorescent protein (tRFP) reporter mice were bled at multiple time points post-infection (Figure S1A). At 8 days post-infection (dpi), the repopulated CD4 T cells in the blood of CD4 T cell-depleted mice did not express IL-21-tRFP, compared with the control group, in which about 5% of CD44⁺CD4 T cells expressed IL-21-tRFP (Figures S1B and S1C). At later time points (22–35 dpi), the frequency of IL-21-tRFP⁺ cells within the activated (CD44⁺) CD4 T cell pool increased in the depleted condition but not to the same frequency as control mice (Figure S1C). Similarly, at 35 dpi, flow cytometric analysis of splenocytes revealed a significantly lower frequency of IL-21-tRFP⁺ cells found within the CD44⁺ CD4 T cells that emigrated to the spleen in the depleted group compared with the control group (Figures S1D–S1F). These data suggest that although IL-21-producing CD4 T cells are capable of emigrating to the spleen following CD4 T cell depletion, their frequency remains low within the pool of activated CD4 T cells. Thus, we next wanted to identify what type of CD4 T cells repopulate in chronically infected mice.

scRNA-seq reveals repopulated CD4 T cells

To characterize the activated CD4 T cells that repopulate following CD4 T cell depletion in LCMV C113 chronic viral infection, we performed scRNA-seq on CD44⁺ CD4 T cells at 21 dpi (Figures 1A and 1B). When visualized by uniform manifold approximation and projection (UMAP), 13 clusters of CD4 T cells were identified (Figure 1C). Top differentially expressed genes and key marker genes were used to identify and characterize these CD4 T cell clusters (Figure 1D). As anticipated, we identified clusters of germinal center Tfh cells (*Cxcr5*^{hi}, *Bcl6*^{hi}, *Il21*, *Pdcd1*^{hi}) and pre-Tfh cells (*Cxcr5*^{int}, *Bcl6*^{int}, *Il21*, *Pdcd1*^{int}, *Cxcr3*), both of which exhibited high IL-21 expression, which is consistent with Tfh cells being the major source of IL-21 during persistent LCMV infection,³ (Figure 1D). Notably, these pre-Tfh and germinal center (GC) Tfh populations exhibited similar transcriptional profiles to LCMV-specific CD4 T cells as we recently profiled using scRNA-seq.³² Interestingly, a population of activated memory (*Klf2*, *Zbtb32*, *Il21*, *Pdcd1*) CD4 T cells, which we have observed in previous studies,²¹ also exhibited high expression of *Il21*. Additionally, in support of our earlier findings (Figure S1), the frequencies of *Il21*-

expressing clusters (GC Tfh, pre-Tfh, and activated memory) were significantly reduced in the CD4 T cell-depletion group (Figure 1E). Of note, the GC Tfh and pre-Tfh clusters expressed the highest levels of *Pdcd1*, followed by the activated memory, *Slamf7^{hi}*, and interferon-stimulatory gene-expressing (ISG) populations (Figure 1D), indicating that these clusters likely consist of virus-specific CD4 T cells, which we recently identified display uniformly high PD-1 expression during LCMV C113.²¹ It is important to note that *Pdcd1* encodes for PD1, which is a coinhibitory receptor, that becomes upregulated following T cell receptor stimulation,³³ particularly in chronic viral infection, where there is chronic antigen exposure.^{34,35} Therefore, *Pdcd1* expression is indicative of antigen-specific T cells in both chronic infection as well as cancer.^{36,37} Surprisingly, a cluster of Th1 cells with low *Pdcd1* expression was predominantly found in the CD4 T cell-depleted condition (Figures 1D and 1E), suggesting that these may be bystander CD4 T cells, which arise in response to the induction of type I interferons during viral infection.³⁸

Meanwhile, other clusters were present at higher frequencies in the CD4 T cell-depleted group compared with in the control group. Specifically, the Th17 cluster (*Rorc*, *Il17a*, *Ccr6*) was almost uniquely identified in the depleted condition, comprising nearly 7% of CD44⁺ CD4 T cells compared with about 1% in the control (Figures 1D and 1E). In addition, multiple *Foxp3^{hi}* Treg populations (*Gzmb⁺* Tregs, *Nr4a1⁺* Tregs, and T follicular regulatory-like cells) were present at higher frequencies in the CD4 T cell-depleted condition compared with the CD4-repleted control (Figure 1E). Interestingly, these clusters were found to have low expression of *Pdcd1* (Figure 1D), suggesting that although they are activated CD44⁺ CD4 T cells, they may not be LCMV specific. These findings suggest that CD4 T cells that repopulate the immune systems of previously CD4 T cell-depleted mice during chronic viral infection consist of more immunoregulatory or immune modulating subsets, such as Tregs and Th17 cells.

Antigen-experienced CD4 T cells also repopulate following CD4 T cell depletion

To further analyze populations of antigen-experienced CD4 T cells, clusters with high expression of *Pdcd1* (activated memory, GC Tfh, pre-Tfh, *Slamf7^{hi}*, and ISG) (Figure 1D) were collectively reclustered (Figure 2A). Key markers were used to characterize and identify these antigen-experienced clusters (Figure 2B). Notably, although there were comparable numbers of total cells per condition (14,286 cells from control and 15,629 cells from CD4 depleted), the majority (68%) of antigen-experienced CD4 T cells were present in control mice compared with in CD4 T cell-depleted mice (Figures 1D, 1E, and 2A). However, there was little difference in the frequencies of Tfh clusters within the antigen-experienced cells from each condition (Figure 2C). Additionally, a distinct cluster of *Irfg*- and granzyme-expressing, antigen-experienced *Pdcd1^{hi}* Th1 cells was found predominantly in the control group (Figures 2A–2C), which was distinct from the bystander *Pdcd1^{lo}* Th1 population identified in Figure 1.

We have previously shown that IL-21-producing CD4 T cells are critical for the generation of effector CD8 T cells in chronic infection and cancer.³ A major CD4 T cell type that produces IL-21 is Tfh cells,²¹ which are significantly reduced in frequency when CD4 T cells are depleted prior to chronic infection, as observed in our scRNA-seq analysis (Figure

1E). Therefore, to further assess the populations of Tfh cells found in CD4 T cell-depleted conditions compared with control, we conducted flow cytometry on splenocytes following LCMV CI13 infection. CD4 T cell-depleted mice had significantly reduced frequencies of Tfh cells (CXCR5⁺ BCL6⁺) within the CD44⁺ CD4 T cell pool, as well as reduced overall numbers of Tfh cells (Figures 2D–2F). These findings validate that there is a diminished Tfh cell response when CD4 T cells repopulate following CD4 T cell depletion during LCMV CI13 infection.

Tfh cell function is known to be important to B cells during infection, especially in GC formation.^{39–41} Therefore, we assessed GC B cells (Figure 2G) and found a significant reduction in the frequency (Figures 2G and 2H) and absolute number (Figure 2I) of CD95⁺GL7⁺ GC B cells, which corroborates previous studies.⁴² These findings support the reduced Tfh cell response and, as a result, GC formation during chronic viral infection found in CD4 T cell-depleted mice.

Immunomodulatory CD4 T cells expand following CD4 T cell depletion

As the CD4 T cells that emigrate to the spleen following depletion were found to have reduced antigen-experienced cells by scRNA-seq analysis, we then turned our focus to the clusters that expressed low levels of *Pdcd1* (Figure 1D). To do this, we reclustered *Pdcd1*^{lo} clusters from Figure 1 (*Klf2* memory, *Gzmb*⁺ Treg, *Nr4a1*⁺ Treg, naive, Tfr-like, T central memory (TCM), Th17, and Th1) (Figures 3A and 3B). Notably, a few clusters were found to be almost exclusive to the CD4 T cell-depleted group, such as the Th17 and *Pdcd1*^{lo} Th1 clusters (Figure 3C). This *Pdcd1*^{lo} Th1 cluster may consist of bystander CD4 T cells, which arise due to type I interferon responses during viral infection,³⁸ and is uniquely distinct from the antigen-experienced *Pdcd1*^{hi} Th1 cluster identified in Figure 2. In addition, populations such as *Gzmb*⁺ Tregs and Tfr-like cells were found at higher frequencies in the depleted condition (Figure 3C). Meanwhile, *Klf2* memory, naive, and *Slamf7*^{hi} cells were present at higher frequencies in the control group (Figure 3C). These findings suggest that an increase in immunomodulatory CD4 T cells may repopulate in CD4 T cell-depleted mice that undergo chronic infection.

We validated this increase in immunomodulatory CD4 T cells that emigrate to the spleen following CD4 T cell depletion and LCMV CI13 infection using flow cytometry. We confirmed that a significantly higher frequency of T regulatory Foxp3⁺ CD44⁺ CD4 T cells repopulated following CD4 depletion and chronic infection compared with controls (Figures 3D and 3E). However, due to significantly lower total numbers of CD4 T cells found in the CD4 T cell-depleted group, the total number of Foxp3⁺ CD44⁺ CD4 T cells found per spleen was lower in the CD4 T cell-depleted mice compared with the control mice (Figure 3F). In addition, a small, yet significant, population of RORγt⁺ CD44⁺ CD4 T cells (Th17 cells) were identified in the CD4 T cell-depleted condition (Figures 3G and 3H); however, this was again not reflected in the total number of Th17 cells per spleen due to significantly fewer numbers of CD4 T cells reconstituted in the CD4 T cell-depleted group (Figure 3I). These findings validate the relatively increased presence of Tregs and Th17 cells that repopulate the CD4 T cell compartment in CD4 T cell-depleted mice during chronic infection.

Adoptive transfer of CD4 T cells fails to rescue the effector CD8 T cell population

As we have previously shown,³ CD4 T cell help via IL-21 production is necessary for effector CD8 T cell differentiation during chronic infection. Additionally, there are significantly fewer IL-21-producing CD4 T cells or Tfh cells, both in frequency and total number, following CD4 T cell depletion (Figures S1, 1D, and 1E). Therefore, we next aimed to determine whether adoptive transfer of *in-vitro*-activated T cell receptor (TCR) transgenic LCMV-specific CD4 T cells (SMARTA cells), which express tRFP when IL-21 is expressed, could rescue effector CD8 T cell formation in chronically infected CD4 T cell-depleted mice (Figure S2A). Although IL-21-tRFP⁺ CD44⁺ CD4 T cells were detected following adoptive transfer (Figures S2B and S2C), they were unable to rescue effector CX₃CR1⁺ CD8 T cell formation (Figures S2D and S2E). Thus, this finding may suggest that the presence of IL-21-producing CD4 T cells in and of itself is not sufficient to support effector CD8 T cell differentiation. One potential explanation is that there may be an issue in the splenic architecture of CD4 T cell-depleted mice, which prevents IL-21-producing CD4 T cells, such as Tfh cells, from homing to the right anatomical location where they can provide the help signals necessary to facilitate effector CD8 T cell differentiation.

ST reveals the distribution of dominant immune cell types

To assess the localization of cells that may play an important role in the effector CD8 T cell response to chronic viral infection that is missing in the absence of CD4 T cell help, we performed 10x Genomic Visium ST on spleens from control and CD4 T cell-depleted mice at 7 and 21 days post-LCMV CI13 infection (Figures 4A and 4B). Following the integration of all sample datasets, a UMAP analysis was conducted, and 7 distinct clusters of 55 μ m spatial spots were identified (Figures 4C and 4D). Clusters were identified based on top differentially expressed genes, which are indicative of the dominant cell types present in the spots from each cluster. Cluster 0 predominantly expressed hemoglobin genes (*Hba-a1* and *Hbb-bs*) as well as myeloid- or macrophage-associated genes (*Retnlg* and *Fcerg*) and was therefore named erythroid/myeloid cells (Figure 4E). Clusters 1 and 2 consisted largely of B cells, although cluster 1 expressed higher *Ighm*, while cluster 2 had higher expression of *Cd19* (Figure 4E). Cluster 3 primarily expressed mitochondrial and ribosomal genes. Interestingly, we found that cluster 4 had the highest expression of *Cd3d*, indicating that the spots within cluster 4 largely contain T cells (Figure 4E). Cluster 5 predominantly expressed genes associated with neutrophils, such as *Ngp*, *S100a9*, *Mpo*, and *Camp* (Figure 4E; data not shown). Various glycoprotein- and platelet-associated genes were expressed by cluster 6. It is important to note some of the limitations with regard to Visium ST, most significantly the large (55 μ m) spot size, which results in reduced resolution of cell types present in each spot. When comparing the breakdown of clusters by sample (Figure 4F), there appeared to be a slight increase in the T cell and B cell clusters and a reduction in the erythroid/myeloid cluster from day 7 samples to day 21 samples, potentially indicating relatively increased white pulp formation over time and decreased red pulp presence.

ST reveals GC loss without CD4 T cell help

Recalling the important role of Tfh cells in GC formation,^{39,40} we assessed key GC B cell-associated markers in our ST data. CD4 T cell-depleted spleens expressed higher levels

of general B cell-associated genes, such as *Cd19* and *Ighd* (Figures 5A and 5B), indicating an increased B cell presence in these spleens compared with control, consistent with what we have observed with flow cytometry (data not shown). However, expression of GC B cell-associated genes, such as *Fas* and *Bcl6*, was significantly reduced in the CD4 T cell-depleted mice (Figures 5A and 5B), supporting our earlier findings of a significant abrogation of GC B cells in this condition (Figures 2G–2I). Additionally, when looking at the expression of these markers by cluster, we found a similar result, with *Bcl6* and *Fas* being more highly expressed in the B cell-dominant clusters (clusters 1 and 2) of control mice compared with CD4 T cell-depleted mice at both time points (Figure 5C). These findings suggest that loss of CD4 T cell help spatially disrupts the formation of GCs, which may result in splenic architectural changes that could potentially contribute to the diminished generation of the effector CD8 T response to viral infection.

CD4 T cell depletion led to an increase in Tregs and reduced *Ii21* expression

As previously shown from our scRNA-seq and flow cytometry analyses (Figure 2), CD4 T cells that repopulate in chronic infection following CD4 T cell depletion have very different phenotypic distributions compared with control mice. To assess the CD4 T cells in this model spatially, we looked at key genes associated with Tregs and Tfh cells. Temporally, we observed an expected reduction in *Cd4* expression at day 7 in CD4 T cell-depleted mice, which bounces back by day 21. Additionally, a large proportion of *Cd4*-expressing spatial spots highly expressed *Foxp3* in the CD4-depletion condition compared with control at 21 dpi (Figures S3A and S3B). Meanwhile, when assessing Tfh cell-associated genes, *Ii21* expression significantly increased over time in the control group but had little to no change in the depleted group (Figures S3C and S3D), in line with our previous findings at the protein level (Figure S1). These data may also suggest a reduced overall Tfh population, consistent with lower *Bcl6* expression levels. However, since *Bcl6* is expressed by both GC B cells and Tfh cells, our analysis would require deconvolution to tease apart the specific cell types present in each spot.

SPOTlight reveals colocalization of Tfh, B, and progenitor CD8 T cells

Although ST offers important insights regarding localization of key genes associated with cell types, the current resolution of this technology (55 μm) makes it challenging to resolve individual cells located in each barcoded spot. Thus, we utilized SPOTlight, a computational tool that deconvolutes ST data using true single cell-transcriptomics data derived from scRNA-seq.⁴³ To do this, we compiled a reference scRNA-seq dataset obtained from multiple studies on various splenocytes (see STAR Methods). After analyzing our reference dataset, we obtained 13 distinct clusters (Figure S4A), which were characterized (Figure S4B) and then used to deconvolute our ST data from 7 (Figures S5A) and 21 (Figure 6A) dpi. SPOTlight analysis generated cell-cell colocalization Pearson correlations among all cell types identified (Figure S6). Interestingly, at 21 dpi, progenitor CD8 T cells ($\text{Ly}108^+\text{TCF1}^{\text{hi}}$) were found to have high localization correlation with Tfh cells in control spleens but not CD4 T cell-depleted spleens (Figures 6C, S6C, and S6D). The potential colocalization of Tfh cells with progenitor CD8 T cells supports our previous findings that IL-21-producing CD4 T cells, and in particular Tfh cells, play a critical role in the differentiation of progenitor CD8 T cells into effector CD8 T cells.^{3,21} In order to visualize

this colocalization, we recolored the SPOTlight-generated spatial plots to focus on three cell types of interest (progenitor CD8 T cells, B cells, and Tfh cells) at 7 (Figures S5B) and 21 (Figure 6B) dpi. At day 7, B cells appear to form follicular clusters, while progenitor CD8 T cells are distributed broadly throughout the spleen (Figure S5B), which may be anticipated due to disruption of the splenic architecture observed during early stages of chronic infection.²⁶ As predicted, at 21 dpi progenitor CD8 T cells were found to colocalize with B cells and Tfh cells in the organized regions (Figure 6B, left). Conversely, progenitor CD8 T cells were found to colocalize with B cells in some disorganized foci at 21 dpi in CD4 T cell-depleted spleens, but the majority of these foci lacked the presence of Tfh cells (Figure 6B, right). These findings suggest that a lack of CD4 T cell help during chronic viral infection may result in further disorganization of the splenic architecture, which may disrupt the colocalization of cell types important in the progenitor to effector CD8 T cell differentiation.

DISCUSSION

In this study, we utilized ST and scRNA-seq to assess the transcriptional landscape and spatial location of activated CD4 T cells under CD4-repleted and CD4-depleted conditions. Notably we identified the colocalization of Tfh cells with progenitor CD8 T cells and B cells, suggesting that this interaction may be critical for the progenitor CD8 T cell differentiation toward effector cells (Figure 6). Our recent works have shown that IL-21-producing CD4 T cells, namely Tfh cells,^{3,21} are important in sustaining effector CD8 T cell responses. Although it has long been established that CXCR5-expressing Tfh cells localize to B cell follicles, particularly GCs,^{44,45} their localization with progenitor CD8 T cells, which also express CXCR5, has not been explored. Our current study revealed that progenitor CD8 T cells are found to colocalize with B cells and Tfh cells in organized regions; however, transient depletion of CD4 T cells results in a disorganized splenic architecture, disrupting this critical colocalization.

The CD4 T cell-depletion model has been extensively utilized when studying persistent viral infection, namely LCMV.^{2,14,15,46–48} In particular, it has been useful in studying CD8 T cell exhaustion due to the established lifelong viremia and high levels of viral persistence.^{2,48} Additionally, the CD4 T cell-depletion model also has broader implications for other chronic infections, such as HIV, where CD4 T cell counts significantly drop,⁴⁹ as well as cancer and the tumor microenvironment, where CD8 T cell exhaustion is also commonly observed.⁵⁰ Although CD4 T cell depletion is commonly used when studying chronic infection, very few studies have assessed the CD4 T cells that repopulate following transient CD4 depletion. Thus, our study provides insight into which CD4 T cell subsets emerge upon repopulation, as well as the potential importance of cellular localization within the splenic architecture, in order to ensure a robust effector CD8 T cell response.

Tfh cells, which predominantly reside in secondary lymphoid organs, such as the spleen and lymph nodes, also provide help that is essential for B cells, thus playing a critical role in GC formation.^{39,40} In addition, other studies have shown that sustained antigen stimulation by GCB cells is important in maintaining Tfh cells⁵¹ and that CD4 T cell and B cell interaction is important for CD4 T cell IL-21 production.⁵² Interestingly, our lab

and others^{7,8,21} have observed CD8 T cells present in close proximity to GCs, suggesting that these CD8 T cells may respond to help provided by Tfh cells at or near GCs. Our deconvoluted ST findings also support this potential colocalization of progenitor CD8 T cells, Tfh cells, and B cells in organized follicular structures by day 21 of chronic infection (Figure 6). In support of this model, a recent study in a preclinical cancer model showed that interaction between neoantigen-driven B cells and Tfh cells is necessary to generate CD8 T cell antitumor responses in an IL-21-dependent manner,⁵³ suggesting that this may be a conserved feature across chronic inflammatory states such as cancer and chronic viral infection. Further exploration of the CXCL13-CXCR5 axis may mechanistically elucidate the interaction of Tfh cells and progenitor CD8 T cells that takes place within specialized structures in B cell follicles identified in this paper.

In addition, our study comparing control and CD4 T cell-depleted chronically infected mice suggests that although IL-21-producing Tfh cells do repopulate following depletion, they are significantly outnumbered by other immunomodulatory CD4 T cells, such as Tregs and even Th17 cells. A critical role of Tregs is to dampen the excessive immune activation that results from chronic infection in an effort to limit tissue disruption.²⁹ Chronic LCMV infection is well documented to cause significant immunopathology and disruption of the splenic architecture,^{25–27} especially in early stages of chronic infection.²⁶ Previous studies have shown a burst of Treg expansion during LCMV C113 infection that peaks at 17 dpi,⁵⁴ which coincides with a return to more organized follicular structures found during the late stage of chronic infection.²⁶ When CD4 T cells are depleted, not only are conventional helper CD4 T cells removed but so are the immunoregulatory CD4 T cells necessary for limiting tissue damage, which may allow for CD8 T cells to expand unregulated²⁶ (Figure S3; *Cd8a* expression) and wreak havoc on the lymphoid tissue. Therefore, it is possible that recent thymic emigrant CD4 T cells in the depletion model have more immunomodulatory roles as they must respond to the splenic tissue disruption caused by an enhanced inflammatory state. It is also important to note that chronic viral infection causes thymic destruction and impaired central tolerance.²⁸ This thymic disruption may also result in diminished reconstitution of CD4 T cells following transient depletion, prior to establishing persistent viral infection. Additionally, impaired central tolerance allows for self-reactive T cells to escape negative selection, which supports an increased immunomodulatory profile of CD4 T cells that arise during chronic infection.

Splenic architectural disruption would also support our observations of the reduced number and frequency of Tfh cells found in CD4 T cell-depleted conditions and Tfh cell inability to colocalize with progenitor CD8 T cells and B cells, as observed on day 21 post-infection. Thus, a lack of splenic structure, including GC formation, upon CD4 T cell depletion may disrupt Tfh cell collaboration with B cells, thereby diminishing Tfh production of IL-21 and ultimately culminating in a loss of progenitor-to-effector CD8 T cell differentiation.

Limitations of the study

In this study, we used expression of *Pdcd1* (gene encoding PD1) as a surrogate marker to identify LCMV-specific CD4 T cells as most GP66-tetramer⁺ cells display high expression of PD-1 and few GP66⁺ cells are available for assessment following CD4-depleted

conditions. However, an important caveat to note is that antigen-experienced T cells may not necessarily be equivalent to LCMV-specific T cells, and future work using alternative approaches, such as new tetramer reagents that encompass additional LCMV CD4-restricted epitopes, may be important to further tease apart the phenotype and differentiation status of CD4 T cells that repopulate following transient CD4 T cell depletion during chronic LCMV infection. With a limited quantity of GP66⁺ CD4 T cells to analyze, it is inconclusive whether the defect in Tfh accumulation following transient CD4 T cell depletion is due to an overall lack of virus-specific CD4 T cells repopulating following transient depletion or a lack of LCMV specificity of returning Tfh cells. Another limitation worth noting is that, currently, there are no commercially available CD4 T cell-depletion antibodies that are effective following the establishment of persistent LCMV infection due to Fc receptor saturation.⁵⁵ In this study, *in vitro* activation was employed to activate and expand SMARTA CD4 T cells prior to transfer into infected mice; of note, *in vivo* activation followed by sorting of infection-matched virus-specific CD4 T cells is another alternative. However, this may potentially require dozens of donor mice per recipient to replicate similar numbers of transferred cells. Another potential caveat to our study of adoptive transfer of virus-specific SMARTA CD4 T cells is that the number of transferred cells may not be robust enough to rescue CD8 T cell exhaustion in CD4 T cell-depleted mice. Thus, it is possible that increasing the number of SMARTA cells transferred may illicit a different CD8 T cell response. Lastly, it is worth noting that with the novelty of ST technology, there is no set “gold standard” analytical approach to ST deconvolution. However, there are many publications and preprint articles reviewing the comparison of multiple deconvolution methods,^{56–58} including SPOTlight,⁴³ the technique used in our study.

STAR★METHODS

RESOURCE AVAILABILITY

Lead contact—Further information and requests for resources and reagents should be directed to and will be fulfilled by the lead contact, Weiguo Cui (weiguo.cui@northwestern.edu).

Materials availability—This study did not generate new unique reagents.

Data and code availability

- Single-cell RNAseq and spatial transcriptomic sequencing data have been deposited at Gene Expression Omnibus (GEO): GSE and are publicly available as of the date of publication. Accession numbers are listed in the key resources table.
- This paper does not report original code.
- Any additional information required to reanalyze the data reported in this paper is available from the lead contact upon request.

EXPERIMENTAL MODEL AND SUBJECT DETAILS

Mice and LCMV CI13 infection—Six- to eight-week-old female C57BL/6 and CD45.1 congenic mice were obtained from the National Cancer Institute grantees program (Frederick, MD). *IL-21 IL-10 IFN- γ* Tri-Reporter mice were generated in our lab, as previously published.²¹ Tri-reporter mice were used due to their ability to express IL-21-turbo red fluorescence protein (IL-21-tRFP). TCR transgenic SMARTA mice were provided by Dr. Noah Butler, University of Iowa, IA, with permission from Dorian McGavern, NINDS, NIH. All mice used in these studies were bred and maintained under the guidelines approved by the Institutional Animal Care and Use Committee (IACUC) of the Medical College of Wisconsin (AUA00003003). LCMV clone 13 (CI13) was intravenously injected at 2×10^6 PFU/mouse to establish chronic infection. CI13 was prepared by a single passage on BHK21 cells.

METHOD DETAILS

Flow cytometry—Lymphocytes were isolated from spleen and blood. Splenocytes from mice were harvested and mashed against a cell strainer to create a single-cell suspension followed by red blood cell lysis (ACK Lysing Buffer, Lonza). Blood was collected in tubes containing sodium citrate and lymphocytes were isolated via gradient centrifugation with LymphoPrep (Stem Cell Technologies, Vancouver, Canada). Cells were then stained with antibodies against cell surface antigens for 30–60 min at 4°C. Transcription factor staining was performed using the True Nuclear transcription factor buffer set (Biolegend, San Diego, CA). Flow cytometry data were acquired on an LSRII or FACSCelesta (BD Biosciences, San Jose, CA, USA) flow cytometer and analyzed using FlowJo (Treestar, Ashland, OR, USA).

Administration of biologics—InVivoMab anti-mouse CD4 (clone GK1.5) antibody was purchased from BioXCell and administered at 500 μ g per mouse at day –1 and +1 post-infection.

LCMV-specific CD4 T cell transfer—Splenocytes were harvested from SMARTA Tri-reporter mice, and CD4 T cells were then enriched using the Stemcell easysep kit. SMARTA CD4 T cells were then activated for three days in wells of a 24-well plate that were coated with α -CD3 (2 μ g/mL) the night before, and cells were cultured in RPMI T cell media under the following Th1-polarizing conditions: α -CD28 (2 μ g/mL), α -IL-4 (1 μ g/mL), IL-2 (10u/mL), and IL-12 (20ng/mL). After three days of culture, *in vitro*-activated SMARTA CD4 T cells were adoptively transferred (~500k/mouse) into congenically marked LCMV CI13-infected recipient mice that were depleted of CD4 T cells one day prior to infection. SMARTA cell transfer took place on day 20 post LCMV CI13 infection, and splenocytes were harvested and analyzed one week later (28 days post-infection, dpi).

Single-cell RNA sequencing and analysis—CD4 T cells were isolated from single-cell suspensions of splenocytes using a negative selection isolation kit (StemCell), then FACS-sorted (see above) for CD44⁺CD4 T cells. 10,000 cells per sample were loaded onto the Chromium Controller (10x Genomics), then the 10x Genomics Chromium Next GEM Single Cell 5' Reagent Kits v2 (Dual Index) was used to generate cDNA and HTO libraries, as described in the manufacturer's protocols. Barcoded libraries were sequenced

on an Illumina NextSeq 500 instrument using a NextSeq 500/550 High Output Kit v2 (150 cycles) (FC-404–2002, Illumina) with the following cycle counts: 28 (read 1), 10 (index 1), 10 (index 2), 90 (read 2). Data were demultiplexed and aligned to the mm10 2020-A reference transcriptome (10x Genomics) using Cell Ranger (v6.0, 10x Genomics). Analysis was performed in R using Seurat (v4.0.6).^{62,63} Number of genes detected per cell and percent mitochondrial genes were plotted, and outliers were removed (number of genes over 2,500 and under 200, and percent mitochondrial genes over 10%) to filter out doublets and dead cells. Samples were integrated and PCA and UMAP were performed using the top 30 principal components.

Visium spatial sequencing and analysis—10 μm sections were generated from frozen spleens using a cryostat and placed on barcoded slides (10x Genomics). The Visium Spatial Gene Expression Slide & Reagent Kit (10x Genomics) was used to generate barcoded cDNA libraries, as described the manufacturer’s protocols. H&E stained tissues on Visium slides were imaged using a Nikon Eclipse Ti2 inverted microscope. Spleen tissue on Visium slides was permeabilized for 18 min to extract mRNA. Barcoded cDNA libraries were sequenced on an Illumina NextSeq 500 instrument using a NextSeq 500/550 High Output Kit v2 (150 cycles) (FC-404–2002, Illumina) with the following cycle counts: 28 (read 1), 10 (index 1), 10 (index 2), 90 (read 2). Loupe Browser (v5.0, 10x Genomics) was used to identify which spatial sequencing capture area spots were in contact with tissue. Demultiplexing and alignment was performed with Space Ranger (v2.1, 10x Genomics) and the mm10 2020-A reference transcriptome (10x Genomics). Analysis was performed in R using Seurat (v4.0.6). Visium datasets were integrated using the SCTransform pipeline, and PCA and UMAP were performed using the top 30 principal components. SPOTlight⁴³ was used to demultiplex Visium data with our integrated reference scRNA-seq data used as a reference.

Deconvolution reference dataset—An integrated scRNA-seq dataset of splenocytes from multiple datasets was used as a reference dataset for SPOTlight deconvolution analysis of spatial transcriptomic data obtained using Visium by 10x Genomics. The following datasets were integrated and used as the reference:

- GP33⁺ CD8 T cells, day 30 post-LCMV C113 infection³ (GSE129139)
- GP33⁺ CD8 T cells, day 33 post-LCMV C113 infection⁵⁹ (GSE201195)
- CD44⁺ CD4 T cells, day 21 post-LCMV C113 infection (Control 1 and CD4 Depleted 1 from this paper: GSE200721)
- Healthy splenocytes from Tabla Muris dataset⁶⁰ (GSE109774)
- B220⁻CD3⁻NK1.1⁻CD11b⁺ myeloid cells day 7 post-LCMV C113 chronic infection⁶¹ (GSE167204)

QUANTIFICATION AND STATISTICAL ANALYSIS

Statistical tests were performed using GraphPad Prism (version 9.0), with data represented as mean \pm SEM. p-values were calculated using two-tailed unpaired Student’s t tests, unless otherwise specified. *p < 0.05, **p < 0.01. in all data shown.

Supplementary Material

Refer to Web version on PubMed Central for supplementary material.

ACKNOWLEDGMENTS

This work is supported by NIH grants AI125741 (W.C.), AI148403 (W.C.), CA246920 (P.T.), AI153537 (R.Z.), and DK127526 (M.Y.K.); by an American Cancer Society (ACS) Research Scholar Grant (W.C.); and by an Advancing a Healthier Wisconsin Endowment (AHW) Grant (W.C.). P.T., M.Y.K., A.B., and S.L. are members of the Medical Scientist Training Program at the Medical College of Wisconsin (MCW), which is partially supported by a training grant from NIGMS (T32-GM080202). R.Z. was also supported by the Cancer Research Institute Irvington Fellowship during this study. This research was completed in part with computational resources and technical support provided by the Research Computing Center at MCW.

REFERENCES

1. Castellino F, and Germain RN (2006). Cooperation between CD4+ and CD8+ T cells: when, where, and how. *Annu. Rev. Immunol.* 24, 519–540. 10.1146/annurev.immunol.23.021704.115825. [PubMed: 16551258]
2. Matloubian M, Concepcion RJ, and Ahmed R (1994). CD4+ T cells are required to sustain CD8+ cytotoxic T-cell responses during chronic viral infection. *J. Virol.* 68, 8056–8063. 10.1128/JVI.68.12.8056-8063.1994. [PubMed: 7966595]
3. Zander R, Schauder D, Xin G, Nguyen C, Wu X, Zajac A, and Cui W (2019). CD4(+) T cell help is required for the formation of a cytolytic CD8(+) T cell subset that Protects against chronic infection and cancer. *Immunity* 51, 1028–1042.e4. 10.1016/j.immuni.2019.10.009. [PubMed: 31810883]
4. Kanev K, Wu M, Drews A, Roelli P, Wurmser C, von Hösslin M, and Zehn D (2019). Proliferation-competent Tcf1+ CD8 T cells in dysfunctional populations are CD4 T cell help independent. *Proc. Natl. Acad. Sci. USA* 116, 20070–20076. 10.1073/pnas.1902701116. [PubMed: 31530725]
5. Utzschneider DT, Charmoy M, Chennupati V, Pousse L, Ferreira DP, Calderon-Copete S, Danilo M, Alfei F, Hofmann M, Wieland D, et al. (2016). T cell factor 1-expressing memory-like CD8(+) T cells sustain the immune response to chronic viral infections. *Immunity* 45, 415–427. 10.1016/j.immuni.2016.07.021. [PubMed: 27533016]
6. Im SJ, Hashimoto M, Gerner MY, Lee J, Kissick HT, Burger MC, Shan Q, Hale JS, Lee J, Nasti TH, et al. (2016). Defining CD8+ T cells that provide the proliferative burst after PD-1 therapy. *Nature* 537, 417–421. 10.1038/nature19330. [PubMed: 27501248]
7. He R, Hou S, Liu C, Zhang A, Bai Q, Han M, Yang Y, Wei G, Shen T, Yang X, et al. (2016). Follicular CXCR5– expressing CD8(+) T cells curtail chronic viral infection. *Nature* 537, 412–428. 10.1038/nature19317. [PubMed: 27501245]
8. Leong YA, Chen Y, Ong HS, Wu D, Man K, Deleage C, Minnich M, Meckiff BJ, Wei Y, Hou Z, et al. (2016). CXCR5(+) follicular cytotoxic T cells control viral infection in B cell follicles. *Nat. Immunol.* 17, 1187–1196. 10.1038/ni.3543. [PubMed: 27487330]
9. Hudson WH, Gensheimer J, Hashimoto M, Wieland A, Valanparambil RM, Li P, Lin JX, Konieczny BT, Im SJ, Freeman GJ, et al. (2019). Proliferating transitory T cells with an effector-like transcriptional signature emerge from PD-1(+) stem-like CD8(+) T cells during chronic infection. *Immunity* 51, 1043–1058.e4. 10.1016/j.immuni.2019.11.002. [PubMed: 31810882]
10. Chen Z, Ji Z, Ngiow SF, Manne S, Cai Z, Huang AC, Johnson J, Staupe RP, Bengsch B, Xu C, et al. (2019). TCF-1-Centered transcriptional network drives an effector versus exhausted CD8 T cell-fate decision. *Immunity* 51, 840–855.e5. 10.1016/j.immuni.2019.09.013. [PubMed: 31606264]
11. Miller BC, Sen DR, Al Aboosy R, Bi K, Virkud YV, LaFleur MW, Yates KB, Lako A, Felt K, Naik GS, et al. (2019). Subsets of exhausted CD8(+) T cells differentially mediate tumor control and respond to checkpoint blockade. *Nat. Immunol.* 20, 326–336. 10.1038/s41590-019-0312-6. [PubMed: 30778252]
12. Beltra JC, Manne S, Abdel-Hakeem MS, Kurachi M, Giles JR, Chen Z, Casella V, Ngiow SF, Khan O, Huang YJ, et al. (2020). Developmental relationships of four exhausted CD8(+) T cell

- subsets reveals underlying transcriptional and epigenetic landscape control mechanisms. *Immunity* 52, 825–841.e8. 10.1016/j.immuni.2020.04.014. [PubMed: 32396847]
13. Snell LM, MacLeod BL, Law JC, Osokine I, Elsaesser HJ, Hezaveh K, Dickson RJ, Gavin MA, Guidos CJ, McGaha TL, and Brooks DG (2018). CD8(+) T cell priming in established chronic viral infection Preferentially directs differentiation of memory-like cells for sustained immunity. *Immunity* 49, 678–694.e5. 10.1016/j.immuni.2018.08.002. [PubMed: 30314757]
 14. Battegay M, Moskophidis D, Rahemtulla A, Hengartner H, Mak TW, and Zinkernagel RM (1994). Enhanced establishment of a virus carrier state in adult CD4+ T-cell-deficient mice. *J. Virol.* 68, 4700–4704. 10.1128/JVI.68.7.4700-4704.1994. [PubMed: 7911534]
 15. Zajac AJ, Blattman JN, Murali-Krishna K, Sourdive DJ, Suresh M, Altman JD, and Ahmed R (1998). Viral immune evasion due to persistence of activated T cells without effector function. *J. Exp. Med.* 188, 2205–2213. 10.1084/jem.188.12.2205. [PubMed: 9858507]
 16. Xin G, Schauder DM, Lainez B, Weinstein JS, Dai Z, Chen Y, Esplugues E, Wen R, Wang D, Parish IA, et al. (2015). A critical role of IL-21-induced BATF in sustaining CD8-T-cell-mediated chronic viral control. *Cell Rep.* 13, 1118–1124. 10.1016/j.celrep.2015.09.069. [PubMed: 26527008]
 17. Elsaesser H, Sauer K, and Brooks DG (2009). IL-21 is required to control chronic viral infection. *Science* 324, 1569–1572. 10.1126/science.1174182. [PubMed: 19423777]
 18. Fröhlich A, Kisielow J, Schmitz I, Freigang S, Shamshiev AT, Weber J, Marsland BJ, Oxenius A, and Kopf M (2009). IL-21R on T cells is critical for sustained functionality and control of chronic viral infection. *Science* 324, 1576–1580. 10.1126/science.1172815. [PubMed: 19478140]
 19. Yi JS, Du M, and Zajac AJ (2009). A vital role for interleukin-21 in the control of a chronic viral infection. *Science* 324, 1572–1576. 10.1126/science.1175194. [PubMed: 19443735]
 20. Chen Y, Zander RA, Wu X, Schauder DM, Kasmani MY, Shen J, Zheng S, Burns R, Taparowsky EJ, and Cui W (2021). BATF regulates progenitor to cytolytic effector CD8(+) T cell transition during chronic viral infection. *Nat. Immunol.* 22, 996–1007. 10.1038/s41590-021-00965-7. [PubMed: 34282329]
 21. Zander R, Kasmani MY, Chen Y, Topchyan P, Shen J, Zheng S, Burns R, Ingram J, Cui C, Joshi N, et al. (2022). Tfh-cell-derived interleukin 21 sustains effector CD8(+) T cell responses during chronic viral infection. *Immunity* 55, 475–493.e5. 10.1016/j.immuni.2022.01.018. [PubMed: 35216666]
 22. Linterman MA, Beaton L, Yu D, Ramiscal RR, Srivastava M, Hogan JJ, Verma NK, Smyth MJ, Rigby RJ, and Vinuesa CG (2010). IL-21 acts directly on B cells to regulate Bcl-6 expression and germinal center responses. *J. Exp. Med.* 207, 353–363. 10.1084/jem.20091738. [PubMed: 20142429]
 23. Zotos D, Coquet JM, Zhang Y, Light A, D’Costa K, Kallies A, Corcoran LM, Godfrey DI, Toellner KM, Smyth MJ, et al. (2010). IL-21 regulates germinal center B cell differentiation and proliferation through a B cell-intrinsic mechanism. *J. Exp. Med.* 207, 365–378. 10.1084/jem.20091777. [PubMed: 20142430]
 24. Rasheed MAU, Latner DR, Aubert RD, Gourley T, Spolski R, Davis CW, Langley WA, Ha SJ, Ye L, Sarkar S, et al. (2013). Interleukin-21 is a critical cytokine for the generation of virus-specific long-lived plasma cells. *J. Virol.* 87, 7737–7746. 10.1128/JVI.00063-13. [PubMed: 23637417]
 25. Borrow P, Evans CF, and Oldstone MB (1995). Virus-induced immunosuppression: immune system-mediated destruction of virus-infected dendritic cells results in generalized immune suppression. *J. Virol.* 69, 1059–1070. 10.1128/JVI.69.2.1059-1070.1995. [PubMed: 7815484]
 26. Mueller SN, Matloubian M, Clemens DM, Sharpe AH, Freeman GJ, Gangappa S, Larsen CP, and Ahmed R (2007). Viral targeting of fibroblastic reticular cells contributes to immunosuppression and persistence during chronic infection. *Proc. Natl. Acad. Sci. USA* 104, 15430–15435. 10.1073/pnas.0702579104. [PubMed: 17878315]
 27. Odermatt B, Eppler M, Leist TP, Hengartner H, and Zinkernagel RM (1991). Virus-triggered acquired immunodeficiency by cytotoxic T-cell-dependent destruction of antigen-presenting cells and lymph follicle structure. *Proc. Natl. Acad. Sci. USA* 88, 8252–8256. 10.1073/pnas.88.18.8252. [PubMed: 1910175]

28. Elsaesser HJ, Mohtashami M, Osokine I, Snell LM, Cunningham CR, Boukhaled GM, McGavern DB, Zúñiga-Pflücker JC, and Brooks DG (2020). Chronic virus infection drives CD8 T cell-mediated thymic destruction and impaired negative selection. *Proc. Natl. Acad. Sci. USA* 117, 5420–5429. 10.1073/pnas.1913776117. [PubMed: 32094187]
29. Belkaid Y, and Tarbell K (2009). Regulatory T cells in the control of host-microorganism interactions (*). *Annu. Rev. Immunol.* 27, 551–589. 10.1146/annurev.immunol.021908.132723. [PubMed: 19302048]
30. Penalzoza-MacMaster P, Kamphorst AO, Wieland A, Araki K, Iyer SS, West EE, O'Mara L, Yang S, Konieczny BT, Sharpe AH, et al. (2014). Interplay between regulatory T cells and PD-1 in modulating T cell exhaustion and viral control during chronic LCMV infection. *J. Exp. Med.* 211, 1905–1918. 10.1084/jem.20132577. [PubMed: 25113973]
31. Provine NM, Badamchi-Zadeh A, Bricault CA, Penalzoza-MacMaster P, Larocca RA, Borducchi EN, Seaman MS, and Barouch DH (2016). Transient CD4+ T cell depletion results in delayed development of functional vaccine-elicited antibody responses. *J. Virol.* 90, 4278–4288. 10.1128/JVI.00039-16. [PubMed: 26865713]
32. Zander R, Khatun A, Kasmani MY, Chen Y, and Cui W (2022). Delineating the transcriptional landscape and clonal diversity of virus-specific CD4+ T cells during chronic viral infection. Preprint at bioRxiv. 10.1101/2022.05.12.491625.
33. Chikuma S, Terawaki S, Hayashi T, Nabeshima R, Yoshida T, Shibayama S, Okazaki T, and Honjo T (2009). PD-1-mediated suppression of IL-2 production induces CD8+ T cell anergy in vivo. *J. Immunol.* 182, 6682–6689. 10.4049/jimmunol.0900080. [PubMed: 19454662]
34. Youngblood B, Oestreich KJ, Ha SJ, Duraiswamy J, Akondy RS, West EE, Wei Z, Lu P, Austin JW, Riley JL, et al. (2011). Chronic virus infection enforces demethylation of the locus that encodes PD-1 in antigen-specific CD8(+) T cells. *Immunity* 35, 400–412. 10.1016/j.immuni.2011.06.015. [PubMed: 21943489]
35. Youngblood B, Noto A, Porichis F, Akondy RS, Ndhlovu ZM, Austin JW, Bordi R, Procopio FA, Miura T, Allen TM, et al. (2013). Cutting edge: prolonged exposure to HIV reinforces a poised epigenetic program for PD-1 expression in virus-specific CD8 T cells. *J. Immunol.* 191, 540–544. 10.4049/jimmunol.1203161. [PubMed: 23772031]
36. Ahmadzadeh M, Johnson LA, Heemskerk B, Wunderlich JR, Dudley ME, White DE, and Rosenberg SA (2009). Tumor antigen-specific CD8 T cells infiltrating the tumor express high levels of PD-1 and are functionally impaired. *Blood* 114, 1537–1544. 10.1182/blood-2008-12-195792. [PubMed: 19423728]
37. Simon S, and Labarriere N (2017). PD-1 expression on tumor-specific T cells: friend or foe for immunotherapy? *OncoImmunology* 7, e1364828. 10.1080/2162402X.2017.1364828. [PubMed: 29296515]
38. Tough DF, Borrow P, and Sprent J (1996). Induction of bystander T cell proliferation by viruses and type I interferon in vivo. *Science* 272, 1947–1950. 10.1126/science.272.5270.1947. [PubMed: 8658169]
39. Crotty S (2014). T follicular helper cell differentiation, function, and roles in disease. *Immunity* 41, 529–542. 10.1016/j.immuni.2014.10.004. [PubMed: 25367570]
40. Crotty S (2011). Follicular helper CD4 T cells (TFH). *Annu. Rev. Immunol.* 29, 621–663. 10.1146/annurev-immunol-031210-101400. [PubMed: 21314428]
41. Weinstein JS, Herman EI, Lainez B, Licona-Limón P, Esplugues E, Flavell R, and Craft J (2016). TFH cells progressively differentiate to regulate the germinal center response. *Nat. Immunol.* 17, 1197–1205. 10.1038/ni.3554. [PubMed: 27573866]
42. Fahey LM, Wilson EB, Elsaesser H, Fistonich CD, McGavern DB, and Brooks DG (2011). Viral persistence redirects CD4 T cell differentiation toward T follicular helper cells. *J. Exp. Med.* 208, 987–999. 10.1084/jem.20101773. [PubMed: 21536743]
43. Elosua-Bayes M, Nieto P, Mereu E, Gut I, and Heyn H (2021). SPOTlight: seeded NMF regression to deconvolute spatial transcriptomics spots with single-cell transcriptomes. *Nucleic Acids Res.* 49, e50. 10.1093/nar/gkab043. [PubMed: 33544846]
44. Breitfeld D, Ohl L, Kremmer E, Ellwart J, Sallusto F, Lipp M, and Förster R (2000). Follicular B helper T cells express CXC chemokine receptor 5, localize to B cell follicles, and support

- immunoglobulin production. *J. Exp. Med.* 192, 1545–1552. 10.1084/jem.192.11.1545. [PubMed: 11104797]
45. Schaerli P, Willimann K, Lang AB, Lipp M, Loetscher P, and Moser B (2000). CXC chemokine receptor 5 expression defines follicular homing T cells with B cell helper function. *J. Exp. Med.* 192, 1553–1562. 10.1084/jem.192.11.1553. [PubMed: 11104798]
 46. Penalzo-MacMaster P, Provine NM, Blass E, and Barouch DH (2015). CD4 T cell depletion substantially augments the rescue potential of PD-L1 blockade for deeply exhausted CD8 T cells. *J. Immunol.* 195, 1054–1063. 10.4049/jimmunol.1403237. [PubMed: 26116499]
 47. Barber DL, Wherry EJ, Masopust D, Zhu B, Allison JP, Sharpe AH, Freeman GJ, and Ahmed R (2006). Restoring function in exhausted CD8 T cells during chronic viral infection. *Nature* 439, 682–687. 10.1038/nature04444. [PubMed: 16382236]
 48. Im SJ, Konieczny BT, Hudson WH, Masopust D, and Ahmed R (2020). PD-1+ stemlike CD8 T cells are resident in lymphoid tissues during persistent LCMV infection. *Proc. Natl. Acad. Sci. USA* 117, 4292–4299. 10.1073/pnas.1917298117. [PubMed: 32034098]
 49. Hazenberg MD, Hamann D, Schuitemaker H, and Miedema F (2000). T cell depletion in HIV-1 infection: how CD4+ T cells go out of stock. *Nat. Immunol.* 1, 285–289. 10.1038/79724. [PubMed: 11017098]
 50. McLane LM, Abdel-Hakeem MS, and Wherry EJ (2019). CD8 T cell exhaustion during chronic viral infection and cancer. *Annu. Rev. Immunol.* 37, 457–495. 10.1146/annurev-immunol-041015-055318. [PubMed: 30676822]
 51. Baumjohann D, Preite S, Reboldi A, Ronchi F, Ansel KM, Lanzavecchia A, and Sallusto F (2013). Persistent antigen and germinal center B cells sustain T follicular helper cell responses and phenotype. *Immunity* 38, 596–605. 10.1016/j.immuni.2012.11.020. [PubMed: 23499493]
 52. Goenka R, Barnett LG, Silver JS, O'Neill PJ, Hunter CA, Cancro MP, and Laufer TM (2011). Cutting edge: dendritic cell-restricted antigen presentation initiates the follicular helper T cell program but cannot complete ultimate effector differentiation. *J. Immunol.* 187, 1091–1095. 10.4049/jimmunol.1100853. [PubMed: 21715693]
 53. Cui C, Wang J, Fagerberg E, Chen PM, Connolly KA, Damo M, Cheung JF, Mao T, Askari AS, Chen S, et al. (2021). Neoantigen-driven B cell and CD4 T follicular helper cell collaboration promotes antitumor CD8 T cell responses. *Cell* 184, 6101–6118.e13. 10.1016/j.cell.2021.11.007. [PubMed: 34852236]
 54. Punkosdy GA, Blain M, Glass DD, Lozano MM, O'Mara L, Dudley JP, Ahmed R, and Shevach EM (2011). Regulatory T-cell expansion during chronic viral infection is dependent on endogenous retroviral superantigens. *Proc. Natl. Acad. Sci. USA* 108, 3677–3682. 10.1073/pnas.1100213108. [PubMed: 21321220]
 55. Wieland A, Kamphorst AO, Valanparambil RM, Han JH, Xu X, Choudhury BP, and Ahmed R (2018). Enhancing FcγR-mediated antibody effector function during persistent viral infection. *Sci. Immunol.* 3, ea03125. 10.1126/sciimmunol.a03125. [PubMed: 30242080]
 56. Chen J, Liu W, Luo T, Yu Z, Jiang M, Wen J, Gupta GP, Giusti P, Zhu H, Yang Y, and Li Y (2022). A comprehensive comparison on cell type composition inference for spatial transcriptomics data. Preprint at bioRxiv. 10.1101/2022.02.20.481171.
 57. Bae S, Na KJ, Koh J, Lee DS, Choi H, and Kim YT (2022). Cell-DART: cell type inference by domain adaptation of single-cell and spatial transcriptomic data. *Nucleic Acids Res.* 50, e57. 10.1093/nar/gkac084. [PubMed: 35191503]
 58. Kleshchevnikov V, Shmatko A, Dann E, Aivazidis A, King HW, Li T, Elmentaite R, Lomakin A, Kedlian V, Gayoso A, et al. (2022). Cell2location maps fine-grained cell types in spatial transcriptomics. *Nat. Biotechnol.* 40, 661–671. 10.1038/s41587-021-01139-4. [PubMed: 35027729]
 59. Kasmani MY, Zander R, Chung HK, Chen Y, Khatun A, Damo M, Topchyan P, Johnson KE, Levashova D, Burns R, et al. (2022). Clonal lineage tracing reveals mechanisms skewing CD8+ T cell fate decisions in chronic infection. *J. Exp. Med.* 220, e20220679. 10.1084/jem.20220679. [PubMed: 36315049]
 60. Tabula Muris Consortium, Supplemental text writing group, Principal investigators, Overall coordination, Logistical coordination, Organ collection and processing, Library preparation and

sequencing, Computational data analysis, Cell type annotation, Writing group (2018). Single-cell transcriptomics of 20 mouse organs creates a Tabula Muris. *Nature* 562, 367–372. 10.1038/s41586-018-0590-4. [PubMed: 30283141]

61. Volberding PJ, Xin G, Kasmani MY, Khatun A, Brown AK, Nguyen C, Stancill JS, Martinez E, Corbett JA, and Cui W (2021). Suppressive neutrophils require PIM1 for metabolic fitness and survival during chronic viral infection. *Cell Rep.* 35, 109160. 10.1016/j.celrep.2021.109160. [PubMed: 34038722]
62. Butler A, Hoffman P, Smibert P, Papalexi E, and Satija R (2018). Integrating single-cell transcriptomic data across different conditions, technologies, and species. *Nat. Biotechnol.* 36, 411–420. 10.1038/nbt.4096. [PubMed: 29608179]
63. Stuart T, Butler A, Hoffman P, Hafemeister C, Papalexi E, Mauck WM 3rd, Hao Y, Stoeckius M, Smibert P, and Satija R (2019). Comprehensive integration of single-cell data. *Cell* 177, 1888–1902.e21. 10.1016/j.cell.2019.05.031. [PubMed: 31178118]

Highlights

- Unique CD4 subsets repopulate in CD4-depleted mice during chronic LCMV infection
- ST shows GC loss and splenic architectural disruption following CD4 depletion
- Tfh cells colocalize with progenitor CD8 T cells and B cells in the spleen
- Transient CD4 depletion disrupts Tfh, progenitor CD8 T, and B cell colocalization

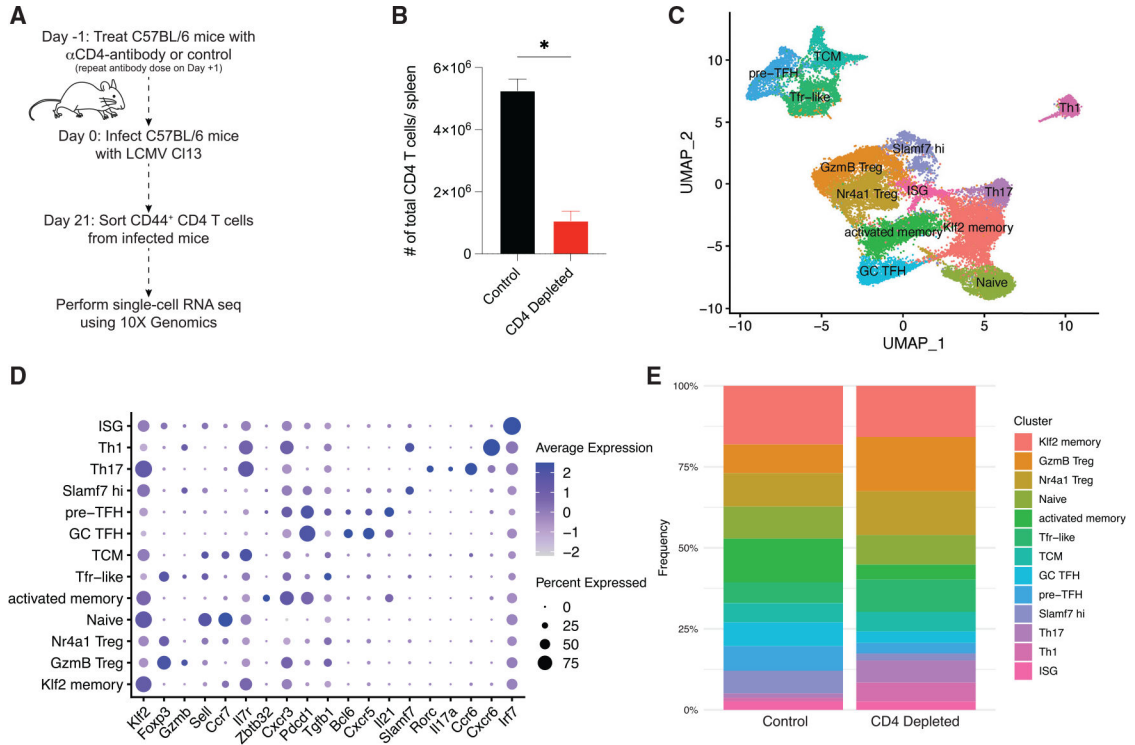


Figure 1. Distinct populations of activated CD4 T cells repopulate the spleens of chronically infected CD4 T cell-depleted mice
 (A) Experimental design where mice were treated with either CD4 T cell-depleting antibody (n = 2) or isotype control (n = 2) and infected with LCMV Cl13. At 21 days post-infection (dpi), splenic CD44⁺ CD4 T cells were fluorescence-activated cell sorted (FACS) and used to perform scRNA-seq using 10x Genomics.
 (B) Total number of CD4 T cells isolated from spleen. Data represented as mean \pm SEM. *p < 0.05.
 (C) UMAP plot from scRNA-seq of CD44⁺ CD4 T cells using Seurat package in R Studio.
 (D) Dot plot depicting expression of key markers used to characterize clusters.
 (E) Cluster breakdown by condition.

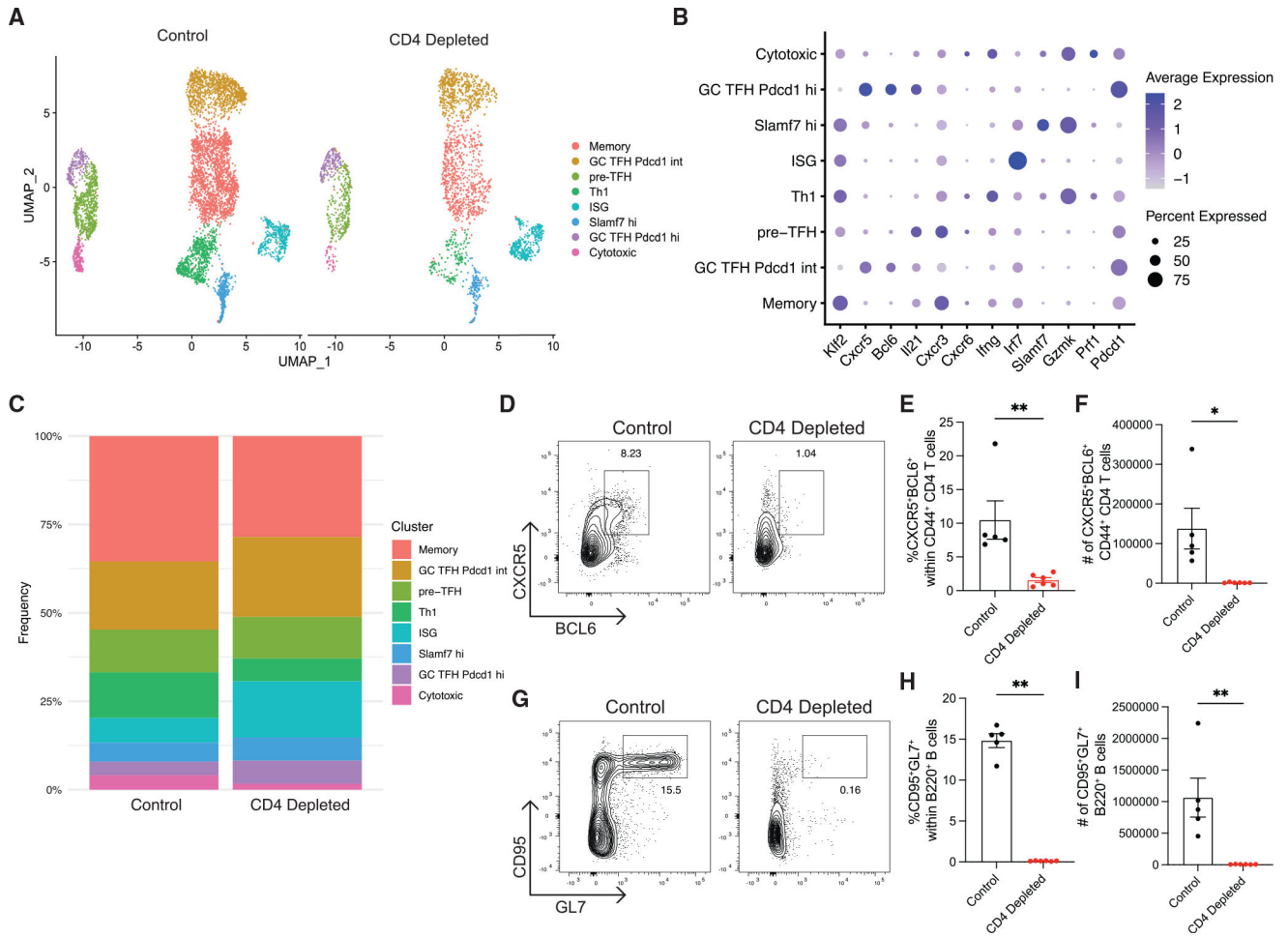


Figure 2. Antigen-experienced CD4 T cells also repopulate following CD4 T cell depletion in chronic infection

(A) UMAP of reclustered *Pdccl1*-expressing populations, depicted in Figure 1D, split by condition. *Pdccl1*-expressing populations were identified as clusters in which over 25% of cells expressed *Pdccl1*.

(B) Dot plot of key markers used to define cluster identities.

(C) Cluster breakdown by condition.

(D) Representative flow plots of CXCR5⁺BCL6⁺ Tfh cells within CD44⁺ CD4 T cells.

(E) Quantified frequency of Tfh cells within CD44⁺ CD4 T cells.

(F) Total number of Tfh cells per spleen.

(G) Representative flow plots of CD95⁺GL7⁺ GCB cells within B220⁺ B cells.

(H) Quantified frequency of GCB cells within B220⁺ population.

(I) Total number of GCB cells per spleen.

Flow cytometry data (D–I) pooled from two independent experiments at 21 and/or 28 dpi.

Data represented as mean ± SEM. *p < 0.05, **p < 0.01.

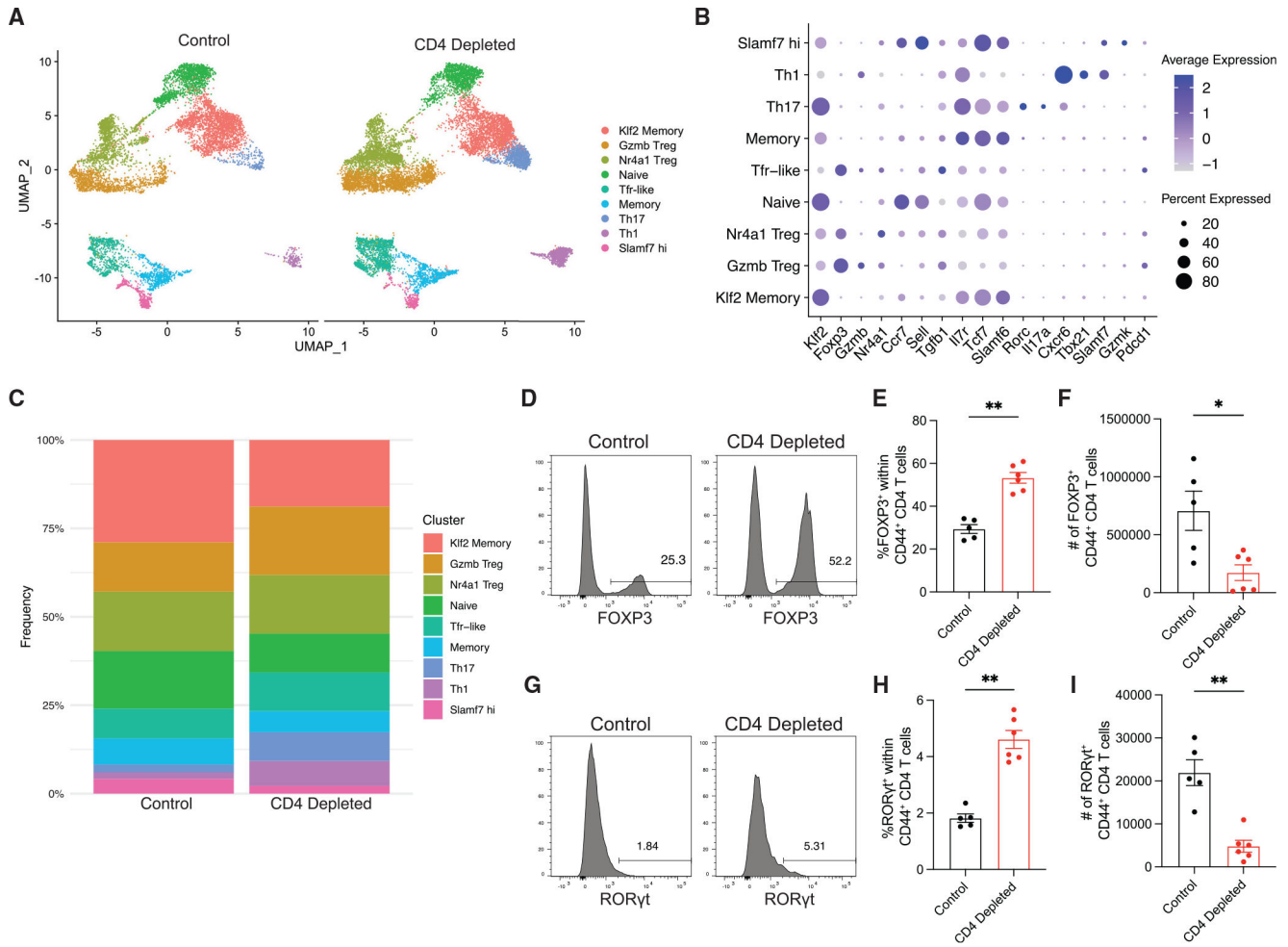


Figure 3. Immunomodulatory CD4 T cells expand following CD4 T cell depletion in chronic infection

(A) UMAP of reclustered *Pcd1*-low populations, depicted in Figure 1D, split by condition.
 (B) Dot plot of key markers used to define cluster identities.
 (C) Cluster breakdown by condition.
 (D) Representative flow plots of FOXP3⁺ Tregs within CD44⁺ CD4 T cells.
 (E) Quantified frequency of Tregs within CD44⁺ CD4 T cells.
 (F) Total number of Tregs per spleen.
 (G) Representative flow plots of RORγt⁺ Th17 cells within CD44⁺ CD4 T cells.
 (H) Quantified frequency of Th17 cells within CD44⁺ CD4 T cell population.
 (I) Total number of Th17 cells per spleen.
 Flow cytometry data (D–I) pooled from two independent experiments at 21 and/or 28 dpi.
 Data represented as mean ± SEM. *p < 0.05, **p < 0.01.

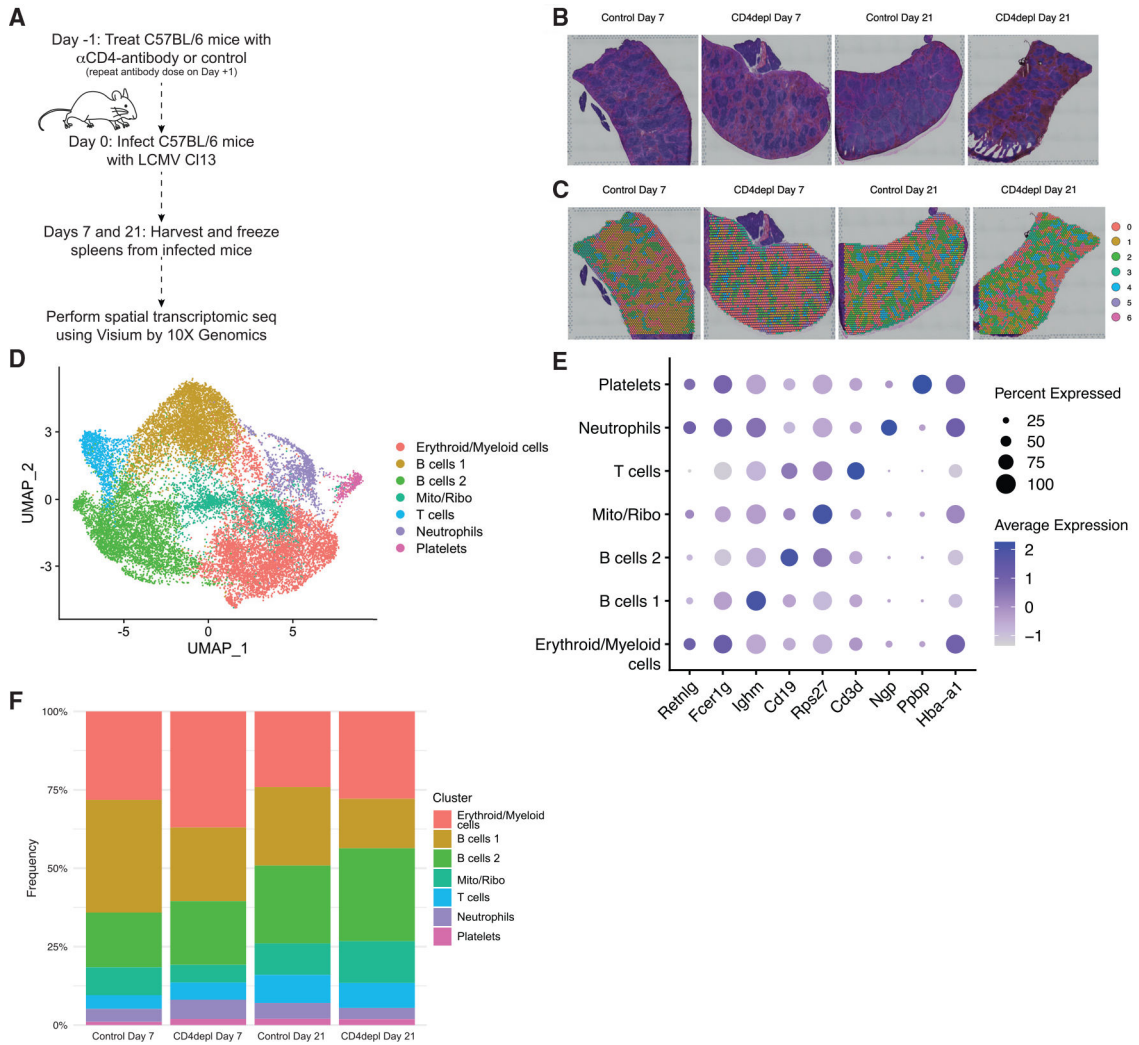


Figure 4. Spatial transcriptomic analysis reveals the distribution of dominant cell types found in the spleens of LCMV CI13-infected control and CD4 T cell-depleted mice
 (A) Experimental design in which spleens from control or CD4 antibody-depleted mice were harvested and frozen at days 7 or 21 post-LCMV CI13 infection and used to perform spatial transcriptomics using Visium by 10x Genomics.
 (B) H&E stain of spleens that underwent spatial transcriptomic sequencing.
 (C) Seven clusters identified following unsupervised clustering overlaid on H&E stained tissue.
 (D) UMAP distribution of the distinct clusters depicted in (C).
 (E) Dot plot of key genes used to identify major cell populations found in respective regions of tissue.
 (F) Breakdown of clusters by sample. One mouse per time point and condition were completed in two independent experiments, n = 2; one representative experiment is shown in the figures.

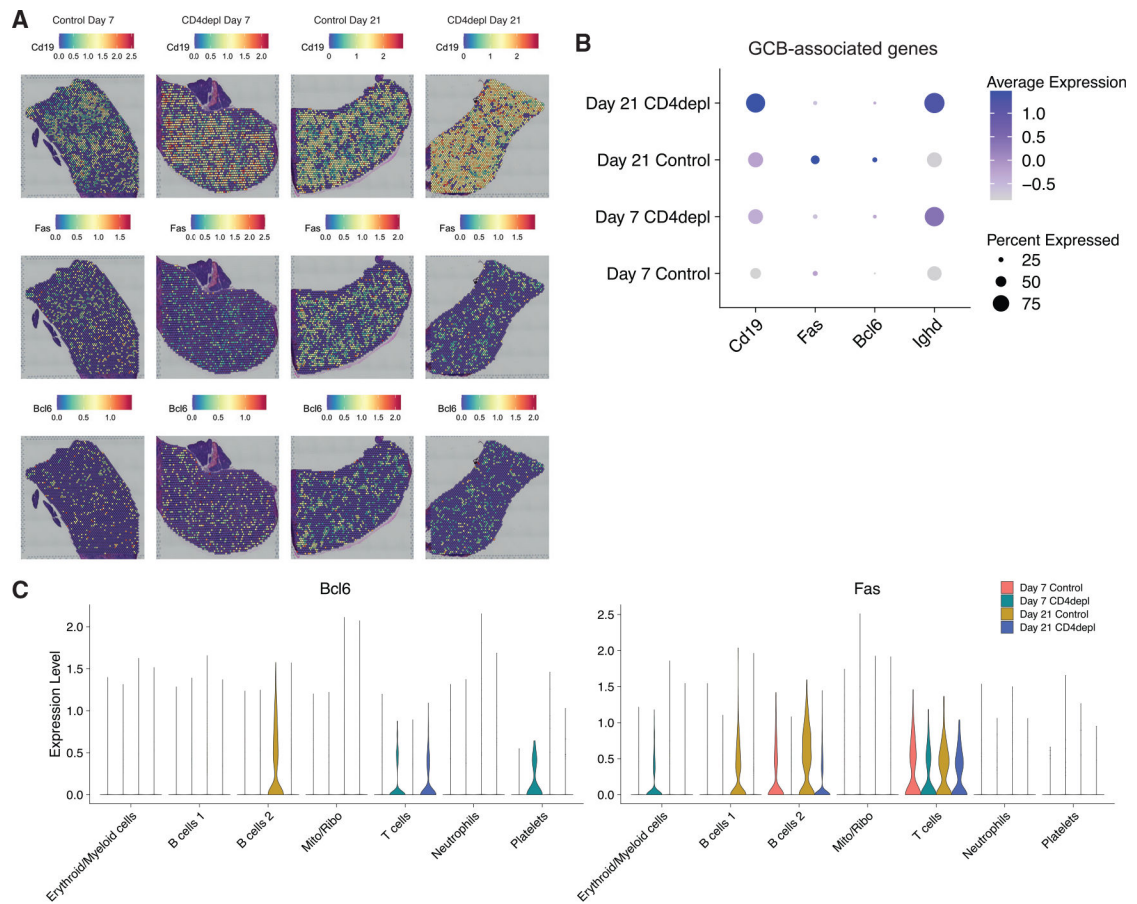


Figure 5. Spatial transcriptomics reveals germinal center loss during chronic infection in the absence of CD4 T cell help

(A) Spatial gene expression of *Cd19*, *Fas*, *Bcl6*, and *Ighd* overlaid on H&E stains of respective tissue.

(B) Dot plot of germinal center and B cell-associated genes.

(C) Violin plot of *Bcl6* and *Fas* broken down by cluster.

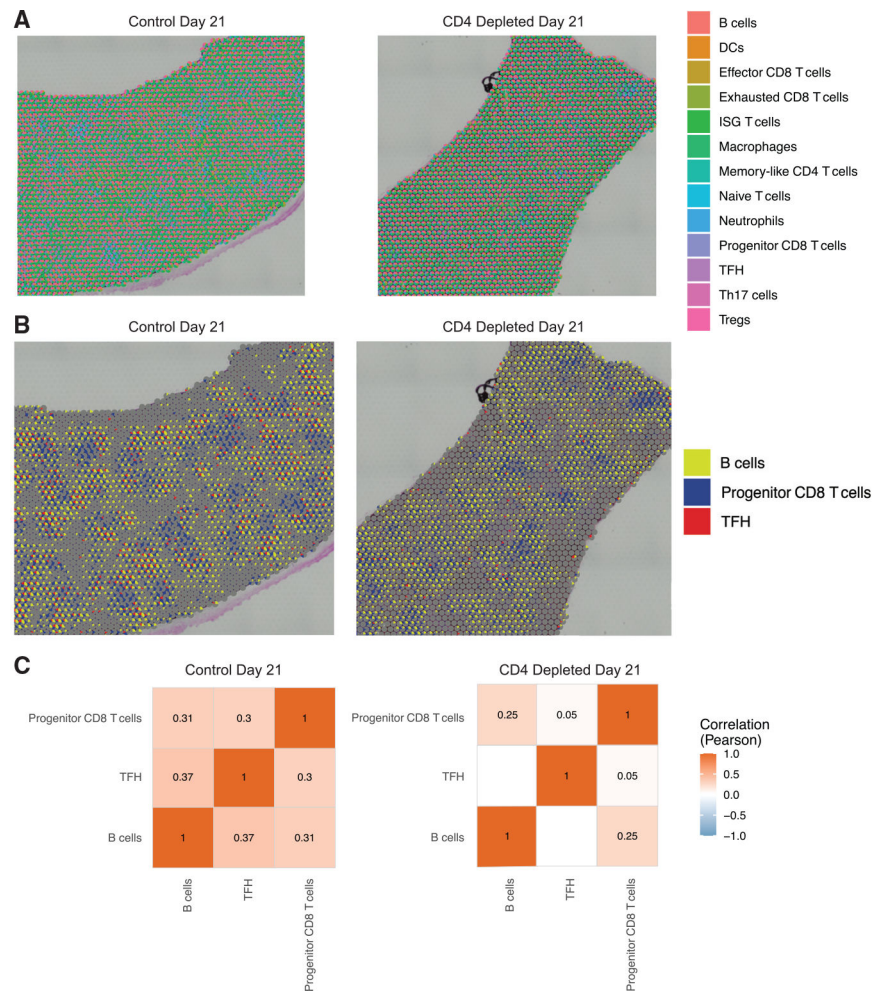


Figure 6. SPOTlight deconvolution reveals colocalization of Tfh cells with progenitor CD8 T cells and B cells

(A) SPOTlight deconvolution scatterplots of spleens from day 21 post-LCMV C113 infection of control and CD4 T cell-depleted mice.

(B) Day 21 SPOTlight scatterplots recolored, showing spatial localization of Tfh cells, progenitor CD8 T cells, and B cells.

(C) Pearson correlation values from SPOTlight deconvolution analysis.

See also Figures S4–S6.

KEY RESOURCES TABLE

REAGENT or RESOURCE	SOURCE	IDENTIFIER
Antibodies		
FITC anti-mouse CD4	BioLegend	Cat#100406, RRID: AB_312691
BV510 anti-mouse/human CD44	BioLegend	Cat# 103044, RRID: AB_2650923
PE/Dazzle 594 anti-mouse CD185 (CXCR5)	BioLegend	Cat# 145522, RRID: AB_2563644
PE/Cyanine7 anti-mouse CD186 (CXCR6)	BioLegend	Cat# 151119, RRID: AB_2721670
PE/Cyanine7 anti-mouse/human CD45R/B220	BioLegend	Cat# 103222, RRID: AB_313005
FITC anti-MU/HU GL7 Antigen (T/B Cell Act. Marker)	BioLegend	Cat# 144604, RRID: AB_2561697
PE anti-mouse CD95 (Fas)	BioLegend	Cat# 152608, RRID: AB_2632902
BV711 anti-mouse CD4	BioLegend	Cat# 100549, RRID: AB_11219396
ROR gamma (t) Monoclonal Antibody (B2D), APC, eBioscience	Thermo Fisher Scientific	Cat# 17-6981-80, RRID: AB_2573253
APC/Cyanine7 anti-mouse CD25	BioLegend	Cat# 102026, RRID: AB_830745
FOXP3 Monoclonal Antibody (FJK-16s), eFluor™ 450, eBioscience	Thermo Fisher Scientific	Cat# 48-5773-82, RRID: AB_1518812
APC/Fire(TM) 750 anti-mouse CD4	BioLegend	Cat# 100460, RRID: AB_2572111
Pacific Blue anti-mouse/human CD44	BioLegend	Cat# 103020, RRID: AB_493683
PerCP anti-mouse CD4	BioLegend	Cat# 100432, RRID: AB_893323
APC/Cyanine7 anti-mouse/human CD44	BioLegend	Cat# 103028, RRID: AB_830785
APC/Fire 750 anti-mouse CD8a	BioLegend	Cat# 100766, RRID: AB_2572113
PE/Cyanine7 anti-mouse CD279 (PD-1)	BioLegend	Cat# 135216, RRID: AB_10689635
PE/Dazzle(TM) 594 anti-mouse CX3CR1	BioLegend	Cat# 149014, RRID: AB_2565698
Pacific Blue(TM) anti-mouse Ly108	BioLegend	Cat# 134608, RRID: AB_2188093
PerCP anti-mouse CD45.1	BioLegend	Cat# 110726, RRID: AB_893345
Pacific Blue(TM) anti-mouse CD45.2	BioLegend	Cat# 109820, RRID: AB_492872
<i>In Vivo</i> MAB anti-mouse CD4	BioCell	Cat#BE0003-1; RRID: AB_1107636
Bacterial and virus strains		
LCMV Clone 13	Rafi Ahmed, PhD	Grown in house
Chemicals, peptides, and recombinant proteins		
LCMV GP33 tetramer	Made in house	N/A
True Nuclear Transcription Factor Buffer Set	Biolegend	Cat#424401
Critical commercial assays		
EasySep Mouse CD4+ T cell isolation Kit	Stem Cell	Cat#19852
Chromium Next GEM Single Cell 5' Kit v2	10× Genomics	Cat# PN-1000244
Chromium Next GEM Single Cell 5' Gel Bead Kit v2	10× Genomics	Cat# PN-1000264
Dynabeads™ MyOne™ SILANE	10× Genomics	Cat# PN-2000048
Library Construction Kit	10× Genomics	Cat# PN-1000190
Chromium Next GEM Chip K Single Cell Kit, 48 rxns	10× Genomics	Cat# PN-1000286

REAGENT or RESOURCE	SOURCE	IDENTIFIER
Dual Index Kit TT Set A	10× Genomics	Cat# PN-1000215
Visium Accessory Kit	10× Genomics	Cat# PN-1000194
Visium Spatial Tissue Optimization Slide & Reagent Kit	10× Genomics	Cat# PN-1000193
Visium Spatial Gene Expression Slide & Reagent Kit	10× Genomics	Cat# PN-1000184
SPRIselect Reagent Kit	Beckman Coulter	Cat#B23318
Kappa NGS quantification kit	KAPABiosystems	Cat#KK4824
NextSeq 500/550 High Output Kit v2.5 (150 cycles)	Illumina	Cat#20024907
Deposited data		
scRNA-seq from CD44 ⁺ CD4 T cells, day 21 post-LCMV C113 infection	This paper	GSE200721
Visium ST of Day 7 and Day 21 post-LCMV C113 infection	This paper	GSE200720
GP33 ⁺ CD8 T cells, day 30 post-LCMV C113 infection	Zander et al. ³	GSE129139
GP33 ⁺ CD8 T cells, day 33 post-LCMV C113 infection	Kasmani et al. ⁵⁹	GSE201195
Healthy splenocytes from Tabla Muris dataset	Tabla Muris et al. ⁶⁰	GSE109774
B220 ⁻ CD3 ⁻ NK1.1 ⁻ CD11b ⁺ myeloid cells day 7 post-LCMV C113 chronic infection	Volberding et al. ⁶¹	GSE167204
Experimental models: Organisms/strains		
C57BL/6 mice	Charles River	N/A
CD45.1 congenic mice	Charles River	N/A
<i>IL-21 IL-10 IFN-γ</i> Tri-Reporter mice	Previous study	Zander et al. ²¹
TCR transgenic SMARTA mice	Noah Butler (UI)	N/A
Software and algorithms		
Cell Ranger 6.0	10× Genomics	https://support.10xgenomics.com/single-cell-gene-expression/software/pipelines/latest/installation
Loupe Browser 5.0	10× Genomics	https://support.10xgenomics.com/spatial-gene-expression/software/visualization/latest/installation
Space Ranger 2.1	10× Genomics	https://support.10xgenomics.com/spatial-gene-expression/software/visualization/latest/installation
SPOTlight 0.1.7	Elosua-Bayes et al. ⁴³	https://github.com/MarcElosua/SPOTlight
Seurat 4.0.6	Butler et al.; Stuart et al. ^{62,63}	https://satijalab.org/seurat/
FlowJo 10.7.1	Tree Star	N/A
Prism 9	Graphpad Software	N/A